A Compartmentalized Hydrogel from a Linear ABC Terpolymer

Rajiv R. Taribagil,[†] Marc A. Hillmyer,*[,‡] and Timothy P. Lodge*[,†]

Department of Chemical Engineering & Materials Science and Department of Chemistry, University of Minnesota, Minneapolis, Minnesota 55455-0431

Received November 8, 2008
Revised Manuscript Received January 8, 2009

The preparation and development of nanostructured colloidal assemblies with high degrees of complexity and organization draws inspiration from biological structures with subdomains on the nanometer length scale.[1] As an example, several groups have realized multicompartment micelles in water or in water−organic solvent mixtures, where incompatible hydrophobic polymers microphase segregate into separate domains in the core.[2−20] The choice of fluorocarbon and hydrocarbon groups as hydrophobic blocks in some of these studies resulted in well-segregated hydrophobic domains, given their high degree of immiscibility. In addition to discrete assemblies such as micelles, it is of equal interest to design multicompartment networks.[21] Weberskirch et al. used living cationic polymerization to synthesize telechelic poly(2-methyl-2-oxazoline) (MOx) with *n*-alkyl and *n*-perfluoroalkyl moieties at the two termini and quantified the segregation of the end groups using NMR spectroscopy at relatively high concentration (∼30 wt % polymer).[22] While this pioneering study clearly showed that the end groups formed separate domains, the morphology of the domains was not resolved. Using poly(2-*n*-nonyl-2-oxazoline) (NOx) and poly(2-(1′*H*,1′*H*,2′*H*,2′*H*-perfluorohexyl)-2-oxazoline) (FOx) as terminal groups with MOx as the hydrophilic block in an ABC triblock terpolymer, Komenda et al. used small-angle neutron scattering (SANS) experiments to obtain more insight into the morphology of the domains.[23] They observed that the scattering curve could be expressed as the sum of intensity profiles obtained from spherical NOx cores and ellipsoidal FOx cores, which led them to infer the presence of a micellar network with spatially separated hydrophobic domains. More recently, Shunmugam et al. prepared lipophilic−hydrophilic−fluorophilic polyacrylate-based ABC triblocks, investigated their behavior in water, and showed that these materials formed hydrogels.[24] However, no morphological characterization was reported in this study.

The purpose of this study is to explore network formation employing hydrophobically modified poly(ethylene oxide) (HM-PEO) with dissimilar terminal groups: poly(1,2 butadiene) (PB) and poly(perfluoropropylene oxide) (PFPO). The polymer chosen for the study is chemically similar to, though architecturally different from, the PEE−PEO−PFPO miktoarm stars previously used to produce multicompartment micelles, which were extensively imaged by cryogenic transmission electron microscopy (cryo-TEM).[5,6,12,14,15] In general, HM-PEO undergoes physical gelation in water at sufficiently high concentrations. Using a variety of hydrophobic alkane groups and poly(alkylene oxide) segments, several groups have mapped the phase behavior for HM-PEO.[25−30] The widely accepted interpretation is that at high concentrations transient networks are formed with the hydrophobic blocks aggregating to form micellar junctions and the hydrophilic PEO stretching to bridge between the junctions. In the case of HM-PEO with two dissimilar and incompatible end groups, the formation of a two-compartment transient network might be expected, as shown in Figure 1.[31] One possible advantage of such a structure is that every PEO midblock is forced to bridge two micelles, and thereby contributing to the network elasticity, in contrast to ABA triblocks in which a significant fraction of midblocks loop back into the same micelle.[32] However, we demonstrate below that the relative strength of the incompatibility among the various blocks and solvent gives rise to a very different structure.

Scheme 1

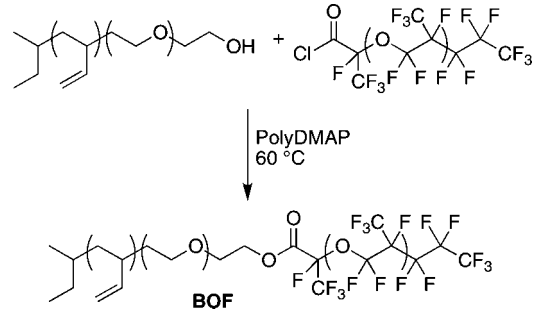

We focus on a solution containing 10 wt % of PB−PEO−PFPO triblock designated BOF(1.9-26-2.3), where the numbers in the parentheses denote the molecular weights of the three blocks in kg mol^{-1}, respectively. Hydroxy-terminated poly(1,2-butadiene)-*b*-poly(ethylene oxide) (BO) diblock copolymer was synthesized by two successive living anionic polymerizations. NMR spectroscopy gave M_n = 1.9 and 26 kg mol^{-1} for PB and PEO, respectively. Carboxylic acid end-capped poly(perfluoropropylene oxide) (PFPO-COOH), with an M_n = 2.3 kg mol^{-1} by ^{19}F NMR spectroscopy, was converted to the acid chloride derivative by reacting with oxalyl chloride. The BOF(1.9-26-2.3) triblock was obtained by coupling the hydroxy end-functional PB−PEO with the acid chloride end-functional PFPO (Scheme 1). A polydispersity index of 1.08 for BOF(1.9-26-

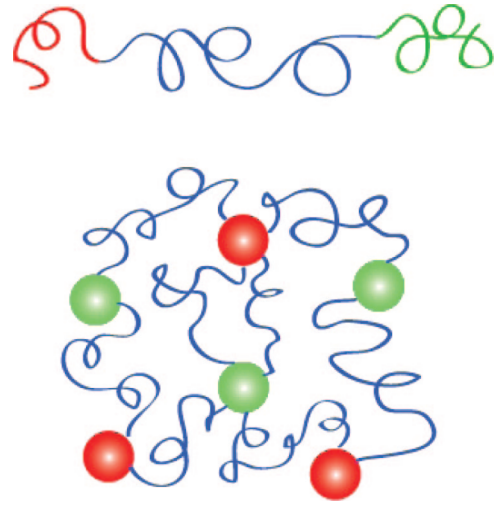

Figure 1. "Expected" morphology of a two-compartment micellar network from association of HM-PEO with two dissimilar end groups in water.

* Authors for correspondence. E-mail: hillmyer@umn.edu, lodge@umn.edu.
† Department of Chemical Engineering & Materials Science.
‡ Department of Chemistry.

10.1021/ma8025089 CCC: $40.75
Published on Web 02/18/2009

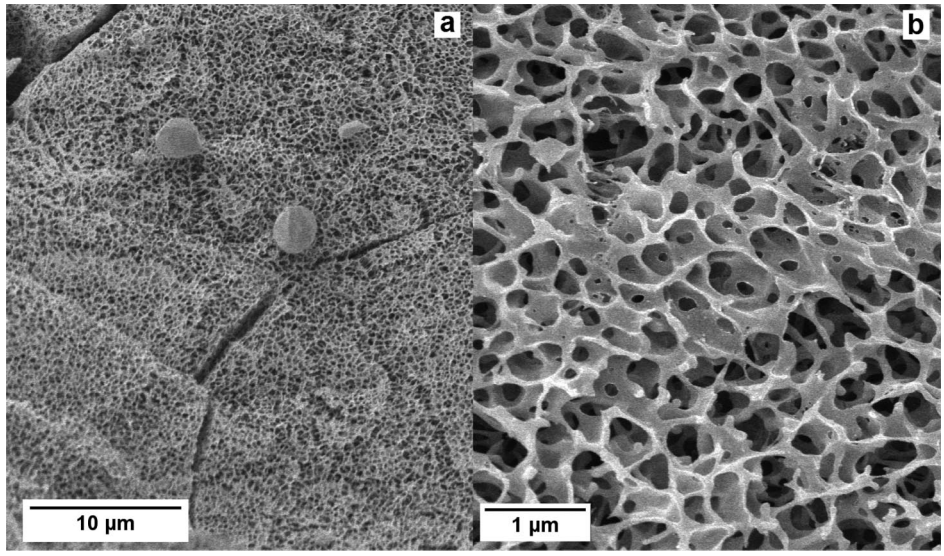

Figure 2. Cryo-SEM micrograph for 10 wt % BOF(1.9-26-2.3) in water at two different magnifications.

2.3) was determined by size exclusion chromatography using polystyrene standards. The volume fractions of PB (f_{PB}), PEO (f_{PEO}), and PFPO (f_{PFPO}) in the copolymer are 0.08, 0.87, and 0.05, respectively. The choice of molecular weights for PB and PFPO was motivated by our previous work on miktoarm stars of the same three components, which involved formation of segregated compartments in the micellar core.[14]

To prepare an aqueous dispersion of BOF(1.9-26-2.3), a film of the desired amount of polymer was hydrated, and the resulting mixture was stirred at 65 °C for 24 h. Mixtures of water (H_2O, Chromasolv grade) and heavy water (D_2O, 99.9% D, Cambridge Isotopes), with compositions varying according to the desired contrast match, were used for SANS experiments. Samples were cooled to RT and stirred for at least 1 week before cryoTEM or SANS characterization. Rheological analysis of this sample showed the dispersion to have a soft solidlike behavior, characteristic of a gel.

Sample preparation for cryo-SEM involved sandwiching a drop of solution between two 0.1 mm deep "freezing hats" and rapidly cooling this assembly using liquid nitrogen jets at an operating pressure of 2100 bar.[33] The assembly was then pried open with a scalpel in a liquid nitrogen bath to fracture the sample longitudinally, allowing a view of its interior. Vitrified water near the surface and a few microns deep into the sample was removed by sublimation at −96 °C and approximately 2×10^{-9} bar for about 5 min. The exposed surface was then coated with an 8 nm thick conducting layer of platinum at −130 °C and then transferred at −150 °C into a Hitachi S900 in-the-lens field emission scanning electron microscope, maintained at about −170 °C. The specimen was imaged using a low acceleration voltage of 2 keV to avoid excessive charging and radiation damage.

For SANS experiments, three different contrast matching H_2O/D_2O mixtures but with same polymer concentration (10 wt %) were prepared. The scattering length density (ρ^*) of the solvent was tuned by mixing H_2O ($\rho^* = -5.6 \times 10^9$ cm^{-2}) and D_2O ($\rho^* = 6.38 \times 10^{10}$ cm^{-2}) to match the scattering length densities for PB, PEO, and PFPO (4.11×10^9, 6.38×10^9, and 4.11×10^{10} cm^{-2}, respectively); see Figure S1 in Supporting Information. Samples were loaded into 1.5 mm quartz banjo cells and exposed to a monochromated neutron beam on the NG-7 30 m instrument of the Cold Neutron Research Facility at the National Institute of Standards and Technology (NIST).[34] Sample-to-detector distances of 1 and 11 m with a neutron wavelength (λ) of 7 Å and a wavelength spread ($\Delta\lambda/\lambda$) of 0.11 were used to cover a range of scattering wave vectors q from 0.0039 to 0.33 Å^{-1}. The resulting data were corrected for background, nonuniform detector efficiency, solvent and empty cell scattering, and sample transmission, using Igor Pro Macros.[35] The scattering intensities were placed on an absolute scale using direct beam flux measurements. The incoherent background was estimated from the asymptotic slope of a Porod plot (Iq^4 vs q^4) and subtracted before data evaluation.[36]

The 10 wt % sample of BOF(1.9-26-2.3) is opaque, suggesting the presence of micron size structures.[37] Cryogenic SEM analysis (Figure 2) reveals a bicontinuous structure with the polymer and water dividing space into two interpenetrating labyrinths. The "pore" (i.e., the previously water-filled chambers) dimensions were 300−700 nm, consistent with the opacity of the solution. The structure is reminiscent of that seen in microporous membranes fabricated using thermally induced phase separation (TIPS), where the membrane structure is a result of separation into a polymer-rich phase and polymer-lean phase.[38−40] We note that the sample did not show any signs of macrophase separation over the course of several weeks. A variety of stable bicontinuous morphologies, of which the most relevant is the sponge phase,[41] have been reported previously for low molecular surfactant systems. Recently, Bates and coworkers reported the existence of a disordered network phase for concentrated aqueous solutions of poly(1,2-butadiene)-*b*-poly(ethylene oxide) (BO) diblock copolymer,[42,33] and the same structure has been inferred for the same diblock in an ionic liquid.[43]

The structure adopted by BOF(1.9-26-2.3) in water is clearly not that depicted in Figure 1. On the contrary, a bicontinuous structure results from the arrangement of the strongly hydrophobic end blocks (PB and PFPO) into space-spanning sheets with nonpreferential curvature, while the PEO chains apparently shield the hydrophobes from water. The proximity of the two hydrophobic blocks in the sheets arises from the strong hydrophobicity of PFPO, which preferentially surrounds itself with another hydrophobe (PB) in an attempt to avoid contact with water. However, given their appreciably high incompatibility, PB and PFPO also segregate into different domains.[5,6,10,13−15,44] This is subject to the constraint that the volume occupied by PB blocks is almost twice that occupied

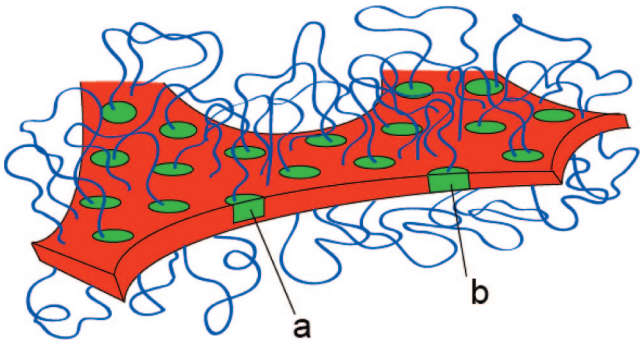

Figure 3. Proposed chain packing motif for the compartmentalized network. PB sheet, PFPO disks, and PEO chains are represented in red, green, and blue, respectively. The PFPO disks could either be (a) thinner than or (b) extend through the PB sheet.

by the PFPO block; an assembly satisfying this constraint would feature domains of PFPO dispersed in a PB matrix. From our previous work, where the formation of disklike fluorodomains was a consistent motif, we propose the shape of the fluoro domains in the hydrophobic sheets to be disklike.[5,6,13−15,45−47]

The process of freeze-drying and water sublimation during SEM sample preparation should cause collapse of the PEO chains onto the hydrophobic sheets. From the SEM micrographs, the thickness of the hydrophobic sheets with the overlying PEO chains was found to range between 35 and 65 nm (after subtracting the thickness of the platinum coating). With 85 vol % of the copolymer being PEO, we approximate the PB + PFPO sheet thickness to be about 5−10 nm. On the basis of these observations, we propose a chain packing arrangement illustrated in the cartoon shown in Figure 3, in which PFPO forms disklike domains within a continuous PB matrix, with PEO chains emanating from each surface.

To assess the viability of the structure depicted in Figure 3, we estimate the associated scattering profile and compare it with the SANS measurements. The complexity of the proposed structure, in terms of the number of components present, the inherent irregularity, and the probable polydispersity with respect to the associated length scales (sheet thickness, disk radius and mean spacing, PEO brush thickness, overall pore size), makes precise prediction of the scattering profile impossible. The solution structure factor contains three "self" contributions coming from each component as well as three pairwise correlations. However, by using contrast matching, the solvent cancels out the coherent contribution from one component; the situation simplifies to three terms (two self-contributions and one pairwise correlation). Furthermore, if one of the two remaining components is the dominant scatterer, the cross-correlation may contribute only weakly. Thus, we posit that a reasonably good prediction can be achieved by including only the individual coherent contributions in the scattering equation.

Given the bicontinuity of the structure, the low q scattering should be dominated by the correlations that exist on the length scale (ξ) of the pore sizes (300−700 nm) estimated from the cryo-SEM micrographs. We describe this correlation using the single length Debye−Anderson−Brumberger (DAB) model for each component.[48] The other contributions to the scattering equation are the form factors for the PFPO disks, the PB sheets, and the PEO brushes as well as an expression to describe the blob scattering from PEO chains;[49,50] eq 1 is the result.

$$\Delta I(q) = (\Delta\rho^*)^2\Big|_{\mathrm{PFPO}}\left\{N\int_0^{\pi/2}[V_{\mathrm{D}}f_{\mathrm{D}}(q)]^2\sin\phi'\,\mathrm{d}\phi' + \frac{8\pi\xi^3(f_{\mathrm{PFPO}}\phi_{\mathrm{polymer}})(1-f_{\mathrm{PFPO}}\phi_{\mathrm{polymer}})}{(1+q^2\xi^2)^2}\right\} + (\Delta\rho^*)^2\Big|_{\mathrm{PB}}\times\left\{\frac{4\pi f_{\mathrm{PB}}\phi_{\mathrm{polymer}}}{\mathrm{d}q^4}\left[1-\cos(qd)\exp\left(\frac{-q^2\sigma_{\mathrm{d}}{}^2}{2}\right)\right] + \frac{8\pi\xi^3(f_{\mathrm{PB}}\phi_{\mathrm{polymer}})(1-f_{\mathrm{PB}}\phi_{\mathrm{polymer}})}{(1+q^2\xi^2)^2}\right\} + (\Delta\rho^*)^2\Big|_{\mathrm{PEO}}\times\left\{\frac{(\psi_{\mathrm{PEO}})^2 f_{\mathrm{PEO}}\phi_{\mathrm{polymer}}}{q^2}[2(L+d/2)\frac{\sin[q(L+d/2)]}{q(L+d/2)}\times\exp\left(\frac{-q^2\sigma_{\mathrm{L}}{}^2}{2}\right) - d\frac{\sin[q(d/2)]}{q(d/2)}\exp\left(\frac{-q^2\sigma_{\mathrm{d}}^2}{2}\right)]^2 + \phi_{\mathrm{polymer}}f_{\mathrm{PEO}}\psi_{\mathrm{PEO}}\xi_{\mathrm{b}}{}^3(1/\mu)\frac{\sin(\mu\arctan(q\xi_{\mathrm{b}}))}{q\xi_{\mathrm{b}}(1+(q\xi_{\mathrm{b}})^2)^{\mu/2}} + \frac{8\pi\xi^3(f_{\mathrm{PEO}}\phi_{\mathrm{polymer}})(1-f_{\mathrm{PEO}}\phi_{\mathrm{polymer}})}{(1+q^2\xi^2)^2}\right\} + \mathrm{Bkgd} \quad (1)$$

The first two terms in eq 1 represent the form factor for the disk-shaped fluoro domains and the single length DAB model to capture the correlation between the disks, respectively. The disk form factor ($f_{\mathrm{D}}{}^2(q)$) is averaged over all orientations by integrating over ϕ', where ϕ' is the angle between the scattering vector q and the normal to the face of the disk (eq 2).

$$\langle f_{\mathrm{D}}{}^2(q)\rangle_{\phi'} = \int_0^{\pi/2}\left[\left(\frac{\sin\left(\frac{qh}{2}\cos\phi'\right)}{\frac{qh}{2}\cos\phi'}\right)\left(\frac{2J_1(qR\sin\phi')}{qR\sin\phi'}\right)\right]^2\sin\phi'\,\mathrm{d}\phi' \quad (2)$$

The next two terms in eq 1, weighted by the scattering length density of PB, correspond to the form factor of the PB sheets and the correlation between them, respectively. The last three terms, weighted by the scattering length density of PEO, include the form factor for the PEO brushes, blob scattering from the PEO chains, and the correlation between the PEO layers, respectively. Given the difficulty in accurately estimating and subtracting the incoherent background scattering, a small background term (Bkgd) has been included in eq 1. The term μ is related to the Flory exponent (υ) by $\mu = 1/\upsilon - 1$, and for PEO in water ($\upsilon = 0.66$[51]), $\mu = 0.515$. ψ_{PEO} represents the volume fraction of PEO in the brush layer diluted by solvent. This can be estimated using the approximation that the ratio of volume of brush layer to that of core scales as the ratio of their thicknesses.[49]

$$\psi_{\mathrm{PEO}} = \frac{\frac{M_{\mathrm{PEO}}/2}{\rho_{\mathrm{PEO}}}}{\frac{M_{\mathrm{PB}}}{\rho_{\mathrm{PB}}}\frac{L}{d/2}} \quad (3)$$

Here d is the thickness of the PB sheet, estimated to be 5 nm from SEM micrographs. The length of the PEO brush layer (L) was estimated by first calculating the blob size (ξ_{b}) for PEO chains emanating from a flat PB sheet (eq 4), an approach adopted by Richter et al.[42] The blob size is equal to the radius corresponding to the area per chain coming out of the sheet; this area is determined by the volume per core block.

$$\xi_{\mathrm{b}} = \left(\frac{2M_{\mathrm{PB}}}{\rho_{\mathrm{PB}}N_{\mathrm{A}}d}\right)^{1/2} \quad (4)$$

Using values for density of PB (ρ_{PB}), Avogadro's number (N_{A}), and the molecular weight of PB (M_{PB}), the blob size was

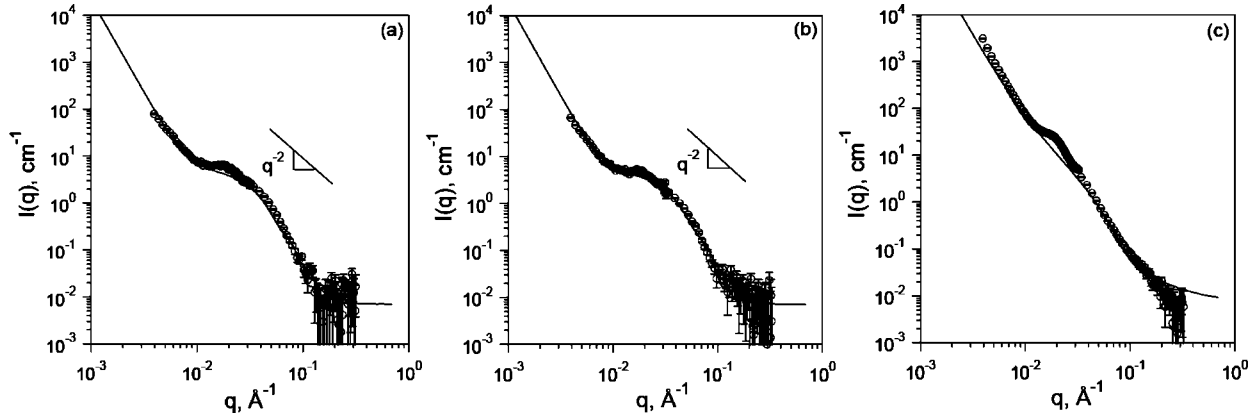

Figure 4. SANS intensity profiles obtained for (a) PB contrast match, (b) PEO contrast match, and (c) PFPO contrast match. The open circles represent experimental data, while the curves represent model predictions.

calculated as 1.2 nm. The number of monomers per blob should be related to the blob size by the law of swollen coils, i.e., PEO chains swollen in water (eq 5).[51,52] A one-dimensional array of blobs makes up the entire chain, and the length of the chain can be given by the product of the number of blobs and the blob length (eq 6).[53]

$$\xi_b = 2R_G = 2(0.215M_{PEO,b}^{0.583})\ \text{Å} \quad (5)$$

$$L = \left(\frac{M_{PEO}}{M_{PEO,b}}\right)\xi_b \quad (6)$$

The standard deviations in the sheet thickness (σ_d) and the brush length (σ_L) were assumed to be 1.5 nm (30%) and 15 nm (30%), respectively. Using the scattering model given in eq 1, we tried to predict the scattering profile for the structure proposed in Figure 3 and compare with our SANS profiles. We found reasonable agreement between the model predictions and experimental data, if 14 nm wide and 5 nm thick PFPO disks were assumed to be embedded in a 5 nm thick PB sheet (Figure 4).

The profiles for PB-matched and PEO-matched conditions are dominated by the PFPO disk form factor in the high q region, as seen from the q^{-2} decay in the intensity, and the DAB correlation in the low q region (see Figures S2, S3, and S4 in Supporting Information). In the PFPO-matched condition, the correlation between PEO brushes dominates at low q while the PB sheet form factor captures the profile at high q. The prediction quality is not as good as seen for other two matches, especially in the high q region, which highlights the need for correlation between contributions from PB and PEO domains.

The transition between the low and high q region is marked by a peak near 0.02 Å^{-1} in all three profiles. If this is a first-order Bragg correlation, the corresponding distance D (= $2\pi/q^*$) is about 30 nm. This is much smaller than the pore size of the network (300−700 nm), which suggests the existence of a correlation within the hydrophobic sheets. From further experiments (not presented here) that indicate the invariance of the peak position with respect to polymer concentration, we propose that the peak corresponds to the spatial correlation that exists between the PFPO disks within the hydrophobic sheet; this is also reasonable given the disk diameter (14 nm).[54]

The sheetlike morphology can be understood in the context of the "superstrong segregation limit" (SSSL), which is accessed when the interfacial tension overwhelms the other contributions to the free energy, leading to the formation of flat interfaces.[46,47,55] The high interfacial tension between PEO/water and PFPO encourages formation of flat disks. In an interesting interplay between PB and PFPO, the fluoro domains surround themselves with PB blocks along the curved surface of the disk to minimize contact with PEO/water (the face of the disk serves as an interface between PFPO and PEO); the incompatibility between PB and PFPO guarantees segregation of both blocks into their respective domains.

The other characteristic that can be anticipated for the SSSL is that the disk thickness should approach twice the fully stretched length (FSL) of the core block. The FSL of PFPO is 5 nm; thus, the disk thickness could be on the order of 10 nm. The value of disk thickness that gave predictions consistent with experimental data (5 nm) is the same as the FSL of PFPO. In the case of 5 nm PFPO disks that expose both faces to the water/PEO interface (i.e., disks that span the PB sheet as shown in (b) of Figure 3), the PFPO blocks either are not completely stretched or are interdigitated, as suggested elsewhere.[46] An alternate possibility would involve having the PB sheet thicker than the PFPO disk, such that only one face of the disk is exposed to water as shown in (a) of Figure 3. In such a case, we would expect to find fully stretched PFPO blocks in the disks; however, it is not possible to distinguish between these two possibilities on the basis of the SANS or cryo-SEM. The FSL of PB is ca. 23 nm, which is much greater than the thickness of sheets, thereby indicating a more relaxed conformation of the PB chains.

In summary, a BOF triblock terpolymer self-assembles into a compartmentalized network, in which fluorocarbon disks (ca. 14 nm in diameter and 5 nm in thickness) are distributed within thin (thickness ~ 5−10 nm) PB sheets. Both faces of the sheet are covered by brushes formed by looping PEO midblocks, and the sheets form a foamlike percolating structure with 300−700 nm pores. This structure is supported by cryo-SEM, SANS, and expectations based on previous studies of multicompartment micelles formed by miktoarm stars of the same three polymers.[5,13−15] However, the structure is quite different from a naive expectation, namely a spatially distinct two compartment micellar network, thereby highlighting the rich structural possibilities available from ABC block terpolymer gels.

Acknowledgment. This work was supported by the MRSEC program of the National Science Foundation under Awards DMR-0212302 and DMR-0819885 at the University of Minnesota. The cryo-SEM experiments were carried out in the University of Minnesota I.T. Characterization Facility, which receives partial support from NSF through the NNIN program. We thank Dr. William F. Edmonds for providing the poly(1,2-butadiene) sample and Chris Frethem for help with the cryo-SEM experiments. We

also acknowledge the help that we received from Dr. Steve Kline and Dr. Paul Butler with the SANS experiments. We also thank Dupont for providing the PFPO-COOH homopolymer.

Supporting Information Available: Calculations of SANS contrast factors and detailed contributions of the various terms in the scattering equation to the overall predictions. This material is available free of charge via the Internet at http://pubs.acs.org.

References and Notes

(1) Lutz, J.-F.; Laschewsky, A. *Macromol. Chem. Phys.* **2005**, *206*, 813–817.
(2) Staehler, K.; Selb, J.; Barthelemy, P.; Pucci, B.; Candau, F. *Langmuir* **1998**, *14*, 4765–4775.
(3) Staehler, K.; Selb, J.; Candau, F. *Langmuir* **1999**, *15*, 7565–7576.
(4) Kotzev, A.; Laschewsky, A.; Adriaensens, P.; Gelan, J. *Macromolecules* **2002**, *35*, 1091–1101.
(5) Li, Z.; Kesselman, E.; Talmon, Y.; Hillmyer, M. A.; Lodge, T. P. *Science (Washington, DC, U.S.)* **2004**, *306*, 98–101.
(6) Lodge, T. P.; Bang, J.; Li, Z.; Hillmyer, M. A.; Talmon, Y. *Faraday Discuss.* **2004**, *128*, 1–12.
(7) Pochan, D. J.; Chen, Z.; Cui, H.; Hales, K.; Qi, K.; Wooley, K. L. *Science (Washington, DC, U.S.)* **2004**, *306*, 94–97.
(8) Kubowicz, S.; Baussard, J.-F.; Lutz, J.-F.; Thuenemann, A. F.; von Berlepsch, H.; Laschewsky, A. *Angew. Chem., Int. Ed.* **2005**, *44*, 5262–5265.
(9) Kubowicz, S.; Thuenemann Andreas, F.; Weberskirch, R.; Moehwald, H. *Langmuir* **2005**, *21*, 7214–9.
(10) Lodge, T. P.; Rasdal, A.; Li, Z.; Hillmyer, M. A. *J. Am. Chem. Soc.* **2005**, *127*, 17608–17609.
(11) Duxin, N.; Liu, F.; Vali, H.; Eisenberg, A. *J. Am. Chem. Soc.* **2005**, *127*, 10063–10069.
(12) Zhu, J.; Jiang, W. *Macromolecules* **2005**, *38*, 9315–9323.
(13) Li, Z.; Hillmyer, M. A.; Lodge, T. P. *Nano Lett.* **2006**, *6*, 1245–1249.
(14) Li, Z.; Hillmyer, M. A.; Lodge, T. P. *Langmuir* **2006**, *22*, 9409–9417.
(15) Li, Z.; Hillmyer, M. A.; Lodge, T. P. *Macromolecules* **2006**, *39*, 765–771.
(16) Thuenemann, A. F.; Kubowicz, S.; Von Berlepsch, H.; Moehwald, H. *Langmuir* **2006**, *22*, 2506–2510.
(17) Cui, H.; Chen, Z.; Zhong, S.; Wooley, K. L.; Pochan, D. J. *Science (Washington, DC, U.S.)* **2007**, *317*, 647–650.
(18) Mao, J.; Ni, P.; Mai, Y.; Yan, D. *Langmuir* **2007**, *23*, 5127–5134.
(19) Fustin, C.-A.; Abetz, V.; Gohy, J.-F. *Eur. Phys. J. E* **2005**, *16*, 291–302.
(20) Hadjichristidis, N.; Iatrou, H.; Pitsikalis, M.; Pispas, S.; Avgeropoulos, A. *Prog. Polym. Sci.* **2005**, *30*, 725–782.
(21) Patrickios, C. S.; Georgiou, T. K. *Curr. Opin. Colloid Interface Sci.* **2003**, *8*, 76–85.
(22) Weberskirch, R.; Preuschen, J.; Spiess, H. W.; Nuyken, O. *Macromol. Chem. Phys.* **2000**, *201*, 995–1007.
(23) Komenda, T.; Luedtke, K.; Jordan, R.; Ivanova, R.; Bonne, T. B.; Papadakis, C. M. *Polym. Prepr. (Am. Chem. Soc., Div. Polym. Chem.)* **2006**, *47*, 763–764.
(24) Shunmugam, R.; Smith, C. E.; Tew, G. N. *J. Polym. Sci., Polym. Chem.* **2007**, *45*, 2601–2608.
(25) Meng, X.-X.; Russel, W. B. *J. Rheol.* **2006**, *50*, 189–205.
(26) Meng, X.-X.; Russel, W. B. *J. Rheol.* **2006**, *50*, 169–187.
(27) Francois, J.; Maitre, S.; Rawiso, M.; Sarazin, D.; Beinert, G.; Isel, F. *Colloids Surf., A* **1996**, *112*, 251–265.
(28) Yang, Y.-W.; Ali-Adib, Z.; McKeown, N. B.; Ryan, A. J.; Attwood, D.; Booth, C. *Langmuir* **1997**, *13*, 1860–1861.
(29) Ricardo, N. M. P. S.; Honorato, S. B.; Yang, Z.; Castelletto, V.; Hamley, I. W.; Yuan, X.-F.; Attwood, D.; Booth, C. *Langmuir* **2004**, *20*, 4272–4278.
(30) Mortensen, K.; Brown, W.; Joergensen, E. *Macromolecules* **1994**, *27*, 5654–66.
(31) Hillmyer, M. A.; Lodge, T. P. *J. Polym. Sci., Polym. Chem.* **2002**, *40*, 1.
(32) Matsumiya, Y.; Matsumoto, M.; Watanabe, H.; Kanaya, T.; Takahashi, Y. *Macromolecules* **2007**, *40*, 3724–3732.
(33) Jain, S.; Dyrdahl, M. H. E.; Gong, X.; Scriven, L. E.; Bates, F. S. *Macromolecules* **2008**, *41*, 3305–3316.
(34) Glinka, C. J.; Barker, J. G.; Hammouda, B.; Krueger, S.; Moyer, J. J.; Orts, W. J. *J. Appl. Crystallogr.* **1998**, *31*, 430–445.
(35) Kline, S. R. *J. Appl. Crystallogr.* **2006**, *39*, 895–900.
(36) Kalur, G. C.; Frounfelker, B. D.; Cipriano, B. H.; Norman, A. I.; Raghavan, S. R. *Langmuir* **2005**, *21*, 10998–11004.
(37) A dilute solution (1 wt %) of this polymer is hazy blue in appearance with dynamic light scattering (DLS) results and cryogenic transmission electron microscopy images revealing 100 nm sized micellar clusters. We attribute this to the presence of dissimilar end groups, which encourages bridging and formation of micellar clusters as compared to looping of the midblock into a single micelle (see ref 31).
(38) van de Witte, P.; Dijkstra, P. J.; van den Berg, J. W. A.; Feijen, J. *J. Membr. Sci.* **1996**, *117*, 1–31.
(39) Bansil, R.; Liao, G. *Trends Polym. Sci.* **1997**, *5*, 146–154.
(40) Nam, Y. S.; Park, T. G. *Biomaterials* **1999**, *20*, 1783–90.
(41) Roux, D.; Coulon, C.; Cates, M. E. *J. Phys. Chem.* **1992**, *96*, 4174–87.
(42) Jain, S.; Gong, X.; Scriven, L. E.; Bates, F. S. *Phys. Rev. Lett.* **2006**, *96*, 138304/1–138304/4.
(43) Simone, P. M.; Lodge, T. P. *Macromolecules* **2008**, *41*, 1753–1759.
(44) Zhu, S.; Edmonds, W. F.; Hillmyer, M. A.; Lodge, T. P. *J. Polym. Sci., Part B: Polym. Phys.* **2005**, *43*, 3685–3694.
(45) Zhou, Z.; Li, Z.; Ren, Y.; Hillmyer, M. A.; Lodge, T. P. *J. Am. Chem. Soc.* **2003**, *125*, 10182–10183.
(46) Edmonds, W. F.; Li, Z.; Hillmyer, M. A.; Lodge, T. P. *Macromolecules* **2006**, *39*, 4526–4530.
(47) Lodge, T. P.; Hillmyer, M. A.; Zhou, Z.; Talmon, Y. *Macromolecules* **2004**, *37*, 6680–6682.
(48) Debye, P.; Anderson, H. R., Jr.; Brumberger, H. *J. Appl. Phys.* **1957**, *28*, 679–83.
(49) Richter, D.; Schneiders, D.; Monkenbusch, M.; Willner, L.; Fetters, L. J.; Huang, J. S.; Lin, M.; Mortensen, K.; Farago, B. *Macromolecules* **1997**, *30*, 1053–1068.
(50) Guinier, A.; Fournet, G. *Small-Angle Scattering of X-rays*; John Wiley and Sons: New York, 1955.
(51) Devanand, K.; Selser, J. C. *Macromolecules* **1991**, *24*, 5943–7.
(52) De Gennes, P. G. *Scaling Concepts in Polymer Physics*; Cornell University Press: Ithaca, NY, 1979.
(53) Halperin, A.; Tirrell, M.; Lodge, T. P. *Adv. Polym. Sci.* **1992**, *100*, 31–71.
(54) Taribagil, R. R.; Hillmyer, M. A.; Lodge, T. P., unpublished results.
(55) Semenov, A. N.; Nyrkova, I. A.; Khokhlov, A. R. *Macromolecules* **1995**, *28*, 7491–500.

MA8025089